Low-Frequency Modes in Nanocrystalline Pd

U. Stuhr
Paul Scherrer-Institut, CH-5232 Villigen PSI, Switzerland

H. Wipf
Institut für Festkörperphysik, Technische Universität Darmstadt, D-64289, Darmstadt, Germany

K. H. Andersen
Institute Laue-Langevin, BP 156X, F-38042 Grenoble Cedex 9, France

H. Hahn
Materialwissenschaften, Technische Universität Darmstadt, D-64287 Darmstadt, Germany
(Received 10 November 1997)

We studied the vibrational modes of H-doped nanocrystalline Pd ($H/Pd \leq 0.04$) by neutron spectroscopy, using the small H content as a probe for a separate determination of the vibrations of Pd atoms at surfaces and/or grain boundaries. We find that these atoms are responsible for the additional low-frequency modes which are characteristic for nanocrystalline materials, and that their local vibrational density of states is essentially linear in frequency. The Pd atoms within grains do not noticeably contribute to the additional low-frequency modes. [S0031-9007(98)06873-2]

PACS numbers: 61.82.Rx, 61.72.Ji, 63.50.+x

The vibrational density of states (VDOS) of nanocrystalline (nano) materials shows, at low frequencies, an increase against coarse-grained material. This increase is established experimentally by neutron [1–5] and resonant nuclear-γ-ray spectroscopy [6], as well as in theoretical calculations [7,8]. However, real atomistic understanding requires knowing whether the additional low-frequency modes in nanostructured materials reflect dominantly vibrations of atoms (i) within grains, (ii) at grain boundaries, or (iii) at surfaces. This question is not answered by the experimental and one of the theoretical [7] studies above since they do not differentiate between (identical) atoms at different local positions. Only a very recent theoretical calculation [8] shows that surface atoms cause in fact low-frequency modes.

This paper reports on a neutron spectroscopy study on two H-doped nano-Pd samples ($H/Pd \leq 0.04$), in which the small H content was a probe for a separate determination of the vibrations of Pd atoms at surfaces and/or grain boundaries. Our results show that these Pd atoms cause additional modes at low frequencies, with a local VDOS essentially linear in frequency, whereas the Pd atoms within grains do not noticeably contribute to these low-frequency modes.

The vibrations of a given atom are described by the spectral density $\langle u^2(\omega, T)\rangle$ of its temperature-dependent vibrational displacements or by its local VDOS $f(\omega)$ (T is the temperature and $\int_0^\infty f(\omega)\, d\omega = 1$). The relation between $\langle u^2(\omega, T)\rangle$ and $f(\omega)$ is [9]

$$\langle u^2(\omega, T)\rangle = f(\omega)\, \frac{3\hbar \coth(\hbar\omega/2k_BT)}{2M\omega}, \qquad (1)$$

where $\hbar$ is Planck's constant, k_B is Boltzmann's constant, and M is the mass of the atom. The total VDOS $F(\omega)$ of a sample is the average of the $f(\omega)$ of all its atoms.

We studied two H-doped nano-Pd samples, a compacted sample prepared by inert gas condensation (IGC Pd, weight 5.4 g, grain size about 17 nm, 2.9 at. % H) and a Pd-black sample (weight 8.3 g, grain size about 4 nm, 4.0 at. % H). For the present small H concentrations, the H of the Pd-black sample is nearly completely located at surfaces [10], whereas it is located at surfaces and/or grain boundaries in the IGC-Pd sample [11,12]. For the latter sample, it is difficult to state reliably the respective fractions of H atoms at surfaces and grain boundaries, although the previous studies assume a dominant trapping at grain boundaries. The light H atoms follow the vibrational motion of the surrounding heavy Pd atoms, so that their low-frequency spectral density $\langle u^2(\omega, T)\rangle$ is almost identical to that of their Pd neighbors (H band modes) [13]. This fact makes H a local probe for the spectral density $\langle u^2(\omega, T)\rangle$ and, according to (1), for the local VDOS $f(\omega)$ of Pd atoms at surfaces and/or grain boundaries.

To determine the spectral density $\langle u^2(\omega, T)\rangle$ of the H (and its Pd neighbors), we separated incoherent and coherent scattering by neutron spin analysis. Since Pd has no spin-incoherent cross section, the incoherent scattering results exclusively from the H, in spite of its low concentration. The incoherent spectrum represents, therefore, via the band modes of the H, also the local VDOS $f(\omega)$ of Pd atoms at surfaces and/or grain boundaries. The coherent scattering, on the other hand, results practically solely from the Pd because of the small H concentrations. It is predominantly determined by Pd atoms within the grains

since their number outweighs by far that of the Pd at surfaces and grain boundaries. Therefore, the incoherent and the coherent spectrums represent the local VDOS $f(\omega)$ of the Pd atoms at surfaces and/or grain boundaries and the total VDOS $F(\omega)$ of the Pd atoms of the entire sample, respectively.

Aside from the low-energy band modes, the H atoms perform high-frequency optical vibrations. For H in a Pd crystal, the energies of these vibrations are above 50 meV [14], and they are even higher for H atoms at grain boundaries and surfaces [10,12]. Vibrations with such high energies are irrelevant for the present experiments.

We report more experimental details now. The IGC-Pd and the Pd-black samples were kept in sealed Al containers. H doping was performed by adding H_2 gas through a valve (3 mbar H_2 gas at 295 K, yielding 2.9 and 4.0 at.% H for IGC Pd and Pd black, respectively). Both samples were in a pure α phase [11,12]. For comparison, we studied also conventional coarse-grained Pb doped with 0.8 at.% H (30 g, again pure α phase).

The neutron scattering data were taken with the time-of-flight spectrometer D7 at the Institute Laue-Langevin. The wavelength of the incident neutrons was 4.84 Å. A bender was used as polarizer, and additional benders could be inserted before the detectors for spin analysis. Our spectra were collected for scattering angles from 55° to 150°. The average flipping ratio determined with a glassy SiO_2 scatterer was 35.6. The samples were mounted in a He-flow cryostat. The scattering from the Al sample container was determined in a separate run (the incoherent Al scattering is in fact negligible because of the extremely small incoherent cross section).

The spin-flip probability for spin-incoherent and coherent scattering is $\frac{2}{3}$ and zero, respectively [15]. This and the known flipping ratio allow transforming the measured non-spin-flip and spin-flip spectra in incoherent and coherent spectra. Figure 1(a) shows the incoherent spectra of the IGC-Pd (280 K) and the Pd-black (260 K) samples, together with the incoherent spectrum of the coarse-grained reference sample (270 K). The three spectra are normalized to equal intensity at $\omega = 0$, and a constant background was subtracted. The background was determined from the inelastic scattering at ~2 K, where all significant neutron energy-gain processes are suppressed. The statistics of the data of the coarse-grained sample are worse than those of the nano samples because of its lower H concentration and the neutron absorption by Pd.

Figure 1(b) shows the data of Fig. 1(a) after division by analyzer transmission and detector efficiency. The spectra in Fig. 1(b) represent, therefore, differential scattering cross sections. The analyzer transmission was determined from a comparison of spectra taken with and without analyzer. The spectra in Fig. 1(b) become quite unreliable for energies above ~20 meV. This results from the low analyzer transmission at high energies and from uncertainties in the background which are irrelevant at low energies. Further, as the time resolution is approximately constant in the investigated energy range, the energy resolution becomes low at high energies. These effects and inelastic scattering from the optic vibrations of the H are the reasons why the intensities in Fig. 1(b) do not decrease at high energies.

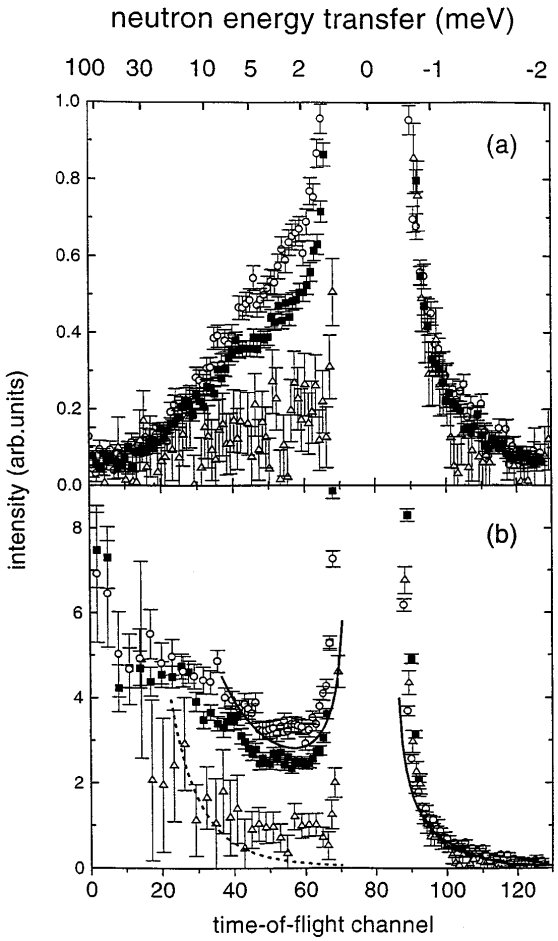

FIG. 1. Spin-incoherent time-of-flight spectra of the IGC-Pd (○, 280 K), Pd-black (■, 260 K), and coarse-grained Pd (△, 270 K) sample. (a) and (b) show the same data without and with correction for analyzer transmission and detector efficiency, respectively. The solid and the dashed lines show spectra for a (local) VDOS proportional to ω and ω^2, respectively.

Figure 2 presents the coherent spectra of the IGC-Pd and the coarse-grained reference sample, together with the spectrum of the empty Al container.

The contribution of an atom to the incoherent scattering is given by the incoherent scattering law $s_{\mathrm{inc}}(\mathbf{Q}, \omega)$, which is the Fourier transform of the time-dependent intermediate scattering law $s_{\mathrm{inc}}(\mathbf{Q}, t)$ ($\hbar\mathbf{Q}$ is the momentum transfer). Assuming randomly orientated crystals and $k_B T \gg \hbar\omega$, we can write [9]

$$s_{\mathrm{inc}}(\mathbf{Q},t) = \exp\left\{-\mathbf{Q}^2 \int_0^\infty d\omega\, f(\omega)\, \frac{k_B T}{M\omega^2}\,[1 - \cos(\omega t)]\right\}, \tag{2}$$

where $f(\omega)$ is the local VDOS of the atom. For the present experimental conditions, the incoherent scattering law is also a fairly good approximation for the inelastic coherent scattering (incoherent approximation). An expansion of (2) yields, after Fourier transformation, the one-phonon approximation for the incoherent scattering law $[f(-\omega) = f(\omega)]$ [9],

$$s_{\mathrm{inc}}(\mathbf{Q},\omega) = \exp\left\{-\mathbf{Q}^2 \int_0^\infty d\omega\, f(\omega)\, \frac{k_B T}{M\omega^2}\right\} \times \left(\delta(\omega) + f(\omega)\, \frac{\mathbf{Q}^2 k_B T}{2M\omega^2}\right). \quad (3)$$

The exponential function is the Debye-Waller factor [16], and $\delta(\omega)$ is the delta function.

Coming back to our data, we find that the incoherent spectra of the two nano samples in Fig. 1(b) differ considerably from the coherent spectra in Fig. 2. The broken and the solid lines in these figures represent the inelastic scattering intensities calculated for $f(\omega)$ [or $F(\omega)$] being proportional to ω^2 and ω, respectively. We can see that the coherent spectra are, at low frequencies, well described by $f(\omega) \propto \omega^2$, a behavior expected for an ordinary three-dimensional material. The solid line in Fig. 1 yields, on the other hand, a fair description of the incoherent spectra of the two nano samples, which shows that $f(\omega)$ of Pd atoms at surfaces and/or grain boundaries is, at low frequencies, essentially linear in ω. This is an important result of the present study. $f(\omega)$ is, for instance, linear in ω if the wave vectors of the contributing phonons are restricted to two dimensions. Our results demonstrate such a linear behavior for both, the Pd-black sample where the H is located at surfaces and the IGC-Pd sample for which H is additionally in grain boundaries.

The above result is confirmed by the data of the coarse-grained sample in Fig. 1(b). In this sample, the H and its Pd neighbors are located within grains. In agreement with this fact, the incoherent spectrum, which reflects $f(\omega)$ of Pd atoms within grains, is distinctly smaller at low energies than the incoherent spectra of the two nano samples and can be described by $f(\omega) \propto \omega^2$.

The coherent spectrum of IGC Pd in Fig. 2 exhibits, at low energies around time-of-flight channel 65, a slightly higher intensity and smaller slope than the coherent spectrum of the coarse-grained sample. This may indicate a small contribution of Pd atoms at surfaces and/or grain boundaries to the total scattering intensity, although it is certainly too small to allow quantitative statements.

Figure 3 shows incoherent spectra of IGC Pd, taken at 2, 200, and 280 K with higher energy resolution than the spectra in Fig. 1 [background determination and correction for detector efficiency and analyzer transmission were the same as in Fig. 1(b)]. The thin solid line indicates the 2 K data. The two thick solid lines represent scattering intensities at 200 and 280 K, calculated according to (2) for a local VDOS $f(\omega)$ of the Pd atoms that is linear in ω up to a cutoff energy $\hbar\omega_{\max} = 12$ meV, and is zero above. The calculations accounted for the experimental energy resolution, and $\omega_{\max}$ was the only adjustable parameter under consideration of the integral scattering intensity.

Figure 4 presents results for the local VDOS $f(\omega)$ as calculated from the 200 and 280 K neutron-energy-gain data of Fig. 3 (positive neutron energy transfers). The solid line shows the linear local VDOS $f(\omega)$ for the

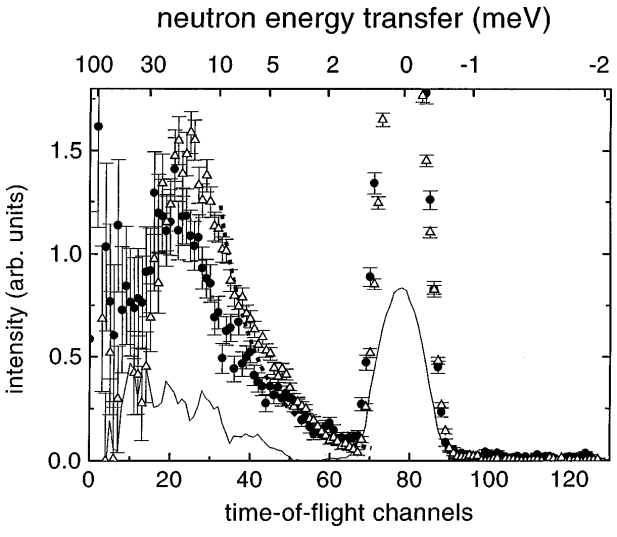

FIG. 2. Coherent spectra of the IGC-Pd (●, 280 K) and the coarse-grained (△, 270 K) samples with correction for analyzer transmission and detector efficiency. The thin solid line is the background of the empty sample container and cryostat. The dashed line is for a VDOS proportional to ω^2.

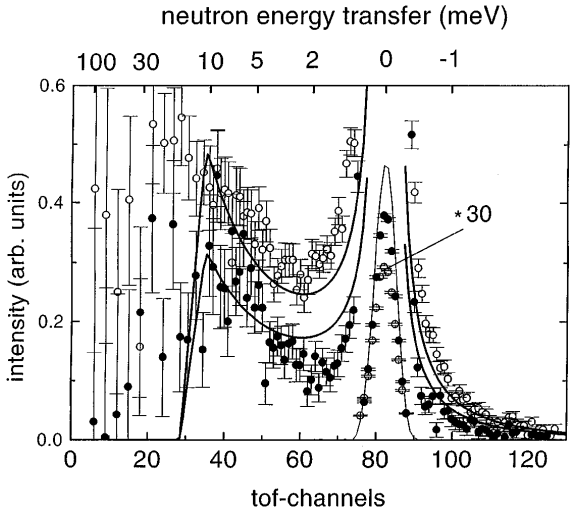

FIG. 3. Incoherent spectra of the IGC-Pd sample at 2 K (thin solid line), 200 K (●), and 280 K (○), corrected for analyzer transmission and detector efficiency. The spectra were taken with higher energy resolution than those of Figs. 1 and 2. The thick solid lines indicate spectra calculated (i) for a local VDOS of Pd atoms proportional to and (ii) for the two sample temperatures 200 and 280 K.

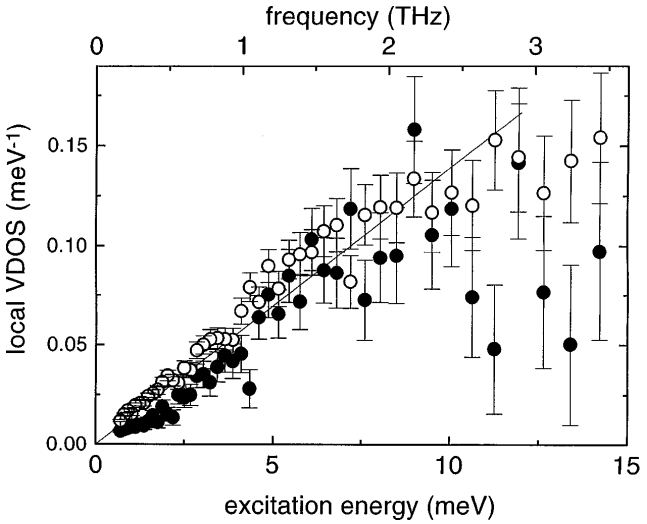

FIG. 4. Local VDOS of Pd atoms calculated from the IGC-Pd spectra in Fig. 3 (● 200 K, ○ 280 K). The solid line stands for a local VDOS linear in ω up to a cutoff energy $\hbar\omega_{\max} = 12$ meV.

Pd atoms as discussed above. The data in Figs. 3 and 4 demonstrate again that a linear ω dependence of $f(\omega)$ provides indeed a satisfactory description of the data, in spite of the simple model assumptions. We mention, finally, that the energy range of the local VDOS (up to 12 meV) agrees well with experimental and theoretical results of the frequencies of the Pd surface atoms [17].

In conclusion, our data for nano-Pd black demonstrate the Pd surface atoms perform low-frequency vibrations with a local VDOS essentially linear in ω. The fact that our nano IGC-Pd data are quite similar shows that Pd atoms at grain boundaries perform comparable vibrations if an appreciable fraction of the H is trapped at grain boundaries as reported in previous studies [11,12]. In both nano samples, the Pd atoms within grains do not noticeably contribute to the additional low-frequency vibrations. Our results for Pd black confirm a recent theoretical study on nano Ag which similarly finds a low-frequency local VDOS of Ag surface atoms that is linear in ω [8].

The authors thank T. Rahman for valuable discussions.

[1] K. Suzuki and K. Sumiyama, Mater. Trans. JIM **36**, 188 (1995).
[2] B. Fultz, L. Anthony, L. J. Nagel, R. M. Nicklow, and S. Spooner, Phys. Rev. B **52**, 3315 (1995).
[3] J. Trampenau, K. Bauszuz, W. Petry, and U. Herr, Nanostruct. Mater. **6**, 551 (1995).
[4] B. Fultz, J. L. Robertson, T. A. Stephens, L. J. Nagel, and S. Spooner, J. Appl. Phys. **79**, 8318 (1996).
[5] H. N. Frase, L. J. Nagel, J. L. Robertson, and B. Fultz, Philos. Mag. B **75**, 335 (1997).
[6] B. Fultz, C. C. Ahn, E. E. Alp, W. Stuhrhahn, and T. S. Toellner, Phys. Rev. Lett. **79**, 937 (1997).
[7] D. Wolf, J. Wang, S. R. Phillpot, and H. Gleiter, Phys. Rev. Lett. **74**, 4686 (1995); J. Wang, D. Wolf, S. R. Phillpot, and H. Gleiter, Philos. Mag. A **73**, 517 (1996).
[8] A. Kara and T. S. Rahman, following Letter, Phys. Rev. Lett. **81**, 1453 (1998).
[9] S. W. Lovesey, *Theory of Neutron Scattering from Condensed Matter* (Clarendon Press, Oxford, 1984), Vol. 1.
[10] J. M. Nicol, J. J. Rush, and R. D. Kelley, Surf. Sci. **197**, 67 (1988).
[11] T. Mütschele and R. Kirchheim, Scr. Metall. **21**, 135 (1987).
[12] U. Stuhr, H. Wipf, T. J. Udovic, J. Weißmüller, and H. Gleiter, J. Phys. Condens. Matter **7**, 219 (1995).
[13] V. Lottner, A. Heim, and T. Springer, Z. Phys. B **32**, 157 (1979); H. R. Schober and V. Lottner, Z. Phys. Chem. **114**, 351 (1979).
[14] T. Springer, in *Hydrogen in Metals I*,Topics in Applied Physics Vol. 28, edited by G. Alefeld and J. Völkl (Springer-Verlag, Berlin, 1978), p. 75.
[15] W. G. Williams, *Polarized Neutrons* (Clarendon Press, Oxford, 1988).
[16] The Debye-Waller factor is zero for a $f(\omega)$ linear in ω. However, the integral scattering intensity is not affected since the integral $\int_{-\infty}^{\infty} s_{\rm inc}(\mathbf{Q}, \omega)\, d\omega = s_{\rm inc}(\mathbf{Q}, t = 0) = 1$ does not change.
[17] W. Zhong, Y. S. Li, and D. Tománek, Phys. Rev. B **44**, 13 053 (1991).